High Data Rate Multiple Input Multiple Output (MIMO) Optical Wireless Communications Using White LED Lighting

Lubin Zeng, *Student Member, IEEE,* Dominic C. O'Brien, *Member, IEEE,* Hoa Le Minh, Grahame E. Faulkner, Kyungwoo Lee, Daekwang Jung, YunJe Oh, Eun Tae Won

***Abstract*—Solid-state lighting is a rapidly growing area of research and applications, due to the reliability and predicted high efficiency of these devices. The white LED sources that are typically used for general illumination can also be used for data transmission, and Visible Light Communications (VLC) is a rapidly growing area of research. One of the key challenges is the limited modulation bandwidth of sources, typically several MHz. However, as a room or coverage space would typically be illuminated by an array of LEDs there is the potential for parallel data transmission, and using optical MIMO techniques is potentially attractive for achieving high data rates. In this paper we investigate non-imaging and imaging MIMO approaches: a non-imaging optical MIMO system does not perform properly at all receiver positions due to symmetry, but an imaging based system can operate under all foreseeable circumstances. Simulations show such systems can operate at several hundred Mbit/s, and up to Gbit/s in many circumstances.**

***Index Terms*—LED, Optical wireless communications, Optical MIMO, Non-Imaging, Imaging Diversity, Blue-filter, Post-equalization.**

I. Introduction

THE LIGHTING industry increasingly employs white-LED devices for illumination and signaling applications. It is thought that such solid-state lighting will eventually replace existing conventional lighting sources due to their reliability and predicted high efficiency. Such sources can also be modulated to provide simultaneous illumination and communication; Visible Light Communications (VLC) was conceived in Japan [1], [2], and there is increasing interest in Europe, including work in a European Commission Framework 7 project OMEGA [3]-[5]. Standardization work is also underway within the IEEE [6].

Illumination is typically provided by an array of LEDs, with levels of 400-800 lux [7] being specified as the minimum required for sufficient illumination. Achieving high data rates is challenging due to the low modulation bandwidth of the sources (several MHz) [8], but the levels of illumination specified for occupation ensure that a very high signal to noise ratio (SNR) is available. The availability of a large number of high SNR channels with low bandwidth makes MIMO techniques an attractive option for achieving high data rates, and the potential of this technique is investigated in this paper.

MIMO is widely used in radio communications [9], where scattering and interference creates channels that are decorrelated from one another. This allows MIMO channels to have higher capacity than their Single Input Single Ouput (SISO) counterparts given a fixed level of total transmission power.

There has been a small amount of research in optical MIMO. Optical channels predominantly use intensity modulation and direct (power) detection, so there is no decorrelation in most cases, and it is only in the case of long atmospheric paths where turbulence and scattering is likely to cause this [10]. For shorter range systems [11] shows a MIMO approach to modelling an indoor system and [12] studied the capacity of a MIMO system, and a low speed demonstration is reported. In [13] work on space-time codes for MIMO is detailed. Reference [14] reports some preliminary experiments with a simple MIMO interconnect. There is also large body of literature on optical interconnects between source and detector arrays (see [15] for a relatively recent review). These examples of parallel free-space optical interconnects typically require precise alignment to map a source to a particular detector or group of detectors and achieve this by design of the physical system. MIMO allows the alignment required for such an interconnect to be achieved 'in the electronics' as it is not necessary that light from a source precisely strikes a single detector. MIMO techniques can used to 'learn' the channel matrix, thus quantifying the crosstalk between the channels created by each source and detector. This can then be used to estimate the transmitted data. The motivation for using MIMO is therefore not for capacity growth, but to reduce the difficulties in achieving alignment physically by using electronic signal processing.

In the application considered here each individual LED has very limited bandwidth, but there are many available for data transmission, but it is not possible to precisely align a detector and receiver array as the receiver moves around the coverage area. MIMO provides an opportunity to do this, and in this paper we consider two 'limiting cases' of receiver types. In the first an array of receivers, each with their own optical

Manuscript received 30 January 2009; revised 15 May 2009. This work was supported by Samsung Electronics Co. ltd., Korea.

Lubin Zeng, Dominc C. O'Brien, Hoa Le Minh, and Grahame E. Faulkner are with the Department of Engineering Science, University of Oxford, Oxford OX1 3PJ, United Kingdom (phone: +44 (0)1865273916, fax: + 44 (0)1865273906 (e-mail: dominic.obrien@eng.ox.ac.uk).

Kyungwoo Lee, Daekwang Jung, YunJe Oh, and Eun Tae Won are with Telecommunication R&D Center, Samsung Electronics Co. Ltd , Suwon, South Korea (phone: +82 (0)312795575, fax: +82 (0)312795255 (e-mail: kyungwoo72.lee@samsung.com).

Digital Object Identifier 10.1109/JSAC.2009.091215.

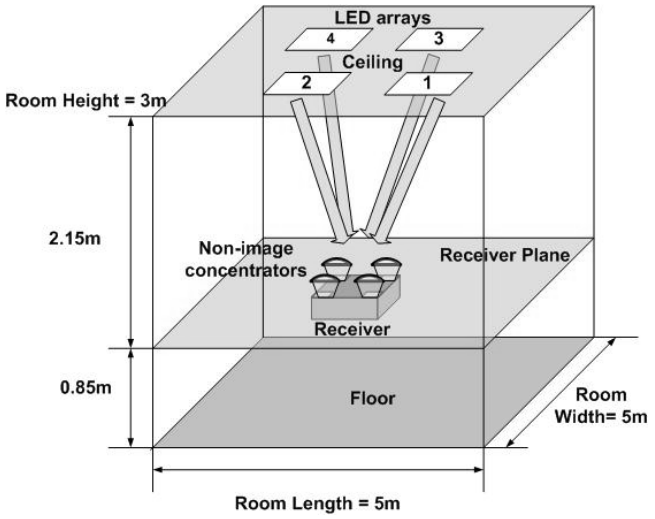

Fig. 1. Non-imaging optical MIMO system

TABLE I
SIMULATION PARAMETERS FOR NON-IMAGING OPTICAL MIMO SIMULATIONS

Parameters	Values
Room size (WxLxH)	5 m x 5 m x 3 m
Number of LEDs arrays	4
Number of LEDs per array	3600(60*60)
LED array pitch	2.5 m
Vertical distance from ceiling to receiving plane d_z	2.15 m
LED pitch	0.01 m
Average transmitted power (per LED)	10 mW
Lambertian order m/Transmitter semi-angle	1/60 deg.
PD responsivityγ (white)	0.4 A/W
Receiver FOV ψ_c (half angle)	62 deg.
Refractive index of optical concentrator n	1.5
Pre-amplifier noise density [17]i_{amp}	5 pA/HZ$^{-1/2}$
Ambient light photocurrent [18]χ_{amb}	10.93 A/m^2/Sr
Receiver Bandwidth B	0.7xNRZ-OOK data rate

concentrator is considered, and in the second an imaging diversity receiver [16] structure is used.

The paper is organized as follows: Section II describes the non-imaging system, together with representative results. In Section III the imaging approach is introduced, and simulated performance presented. Section IV describes the effect of misalignments on system design, Section V discusses aspects of system operation and Section VI draws conclusions from the paper.

II. NON-IMAGING OPTICAL MIMO SYSTEM

Fig. 1 shows a non-imaging optical MIMO system, in a geometry that is based on that used in [1]. Four LED arrays are used to illuminate the room, each of which transmits an independent data stream simultaneously. A four element receiver is used, and each element has an individual non-imaging concentrator. These are arranged in a 2x2 array on a 0.1 m pitch.

Light from each of the LED arrays is received by all the separate receivers, but with different strengths. System performance is calculated at a number of different positions, using the method described in the following sections (Note that a four channel system is used as an example for explanation and for the general case analysed below it is assumed that the system has N_T transmitters and N_R receivers). Other parameters used in the simulations are shown in Table I. It is also assumed that the transmitter operation is coordinated by a controller, and the channel matrix is known at the receiver, in order that the signal can be recovered. Methods to achieve this and other aspects of the operation of a practical system are discussed in section V.

A. Non-imaging optical MIMO Model

A schematic of the system model is shown in Fig. 2, and each of the components is described in the following sections.

B. Transmitter

The transmitter consists of a number of white LEDs [19]. These use a blue LED emitter that excites a yellow phosphor to create a resulting white emission. For the white emission, the slow response of the phosphor limits the modulation bandwidth to approximately 2.5 MHz [20] for the Luxeon devices. Improved modulation bandwidth (typically 14 MHz [20]) can be achieved by using only the blue emission component (usually by placing a blue optical filter at the receiver), although this blocks a significant amount of the emitted energy. Alternatively a receiver equalizer [8] can be used to compensate for the source, and bandwidths of 50 MHz have been simulated using this technique (Note that this is not compensating for the channel, as in previous approaches [21], but for the source, so a simple fixed single-pole equalizer is adequate). Typical data rates available are 12, 30 and 40 Mbit/s for the white, blue and equalized SISO channels using Non-Return to Zero On-Off Keying (NRZ-OOK). There are, however penalties to be considered. For the equalized case there is an SNR penalty of approximately 18 dB (electrical) due to the equalizer [8], and for the blue filtering approximately 10% of the power is in the blue emitted component, the detectors have lower responsivity, and filters typically have transmissions of 60%. This leads to a penalty of 36 dB(electrical) compared with the white channel.

At present it is unclear what modulation scheme is best for the high SNR low bandwidth channel that visible light communications (VLC) offers. In [4] complex multilevel schemes are used, and in [20] equalized Non-Return to Zero On-Off Keying (NRZ-OOK) is used. In this case we consider NRZ-OOK, due to its simplicity and promising results, although the MIMO technique is not limited to any particular modulation scheme.

The system input is a serial transmitted data stream, which is converted into a number of parallel streams, corresponding to the number of transmitters N_T. In the simulation a random NRZ-OOK bit-stream is generated, and this is converted into a vector representing a time-domain waveform, with 10 samples used for each bit.

Each of these individual data streams is then convolved with the measured impulse response [8] of the LED $h_{LED}(t)$ for the particular type of channel (white or blue) being simulated. At a particular instant in time a vector $T = [t_1, ...t_i..t_{N_T}]^T$ is transmitted, where t_i is the convolution of the ith parallel

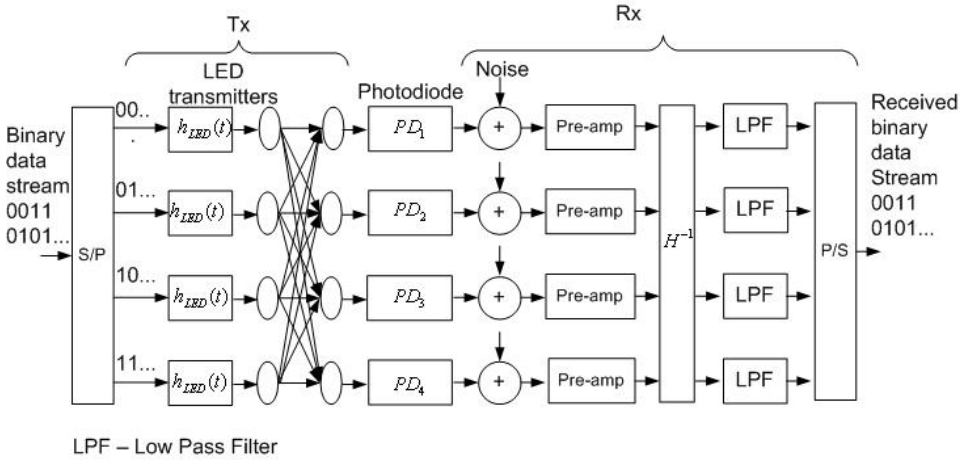

Fig. 2. Schematic of non-imaging optical MIMO model

binary data stream with the LED impulse response, and $[..]^T$ represents transpose.

It is assumed that an LED has a Lambertian radiant intensity (measured in W/sr).

$$R_o(\phi) = [(m+1)/2\pi]\cos^m(\phi), \tag{1}$$

where m is the order of Lambertian emission, and ϕ is the angle of emission relative to the optical axis of the emitter. The average power used for communications is P_{LED}, and it is assumed that the LEDs are fully modulated (i.e. that the instantaneous emitted power ranges from 0 to $2P_{LED}$).

C. Calculating the H matrix

Light propagates from each of the LEDs to the receiver, and there are generally two types of propagation. Each LED has a line-of-sight (LOS) component that propagates to the receiver, and there is also a diffuse component to that propagates via reflections from the surfaces within the room. Simulations of equivalent single channel systems (reported in [8]) indicated that the diffuse component is strongest (relative to the LOS components) when the receiver was in the corner of the room, and that it was at least 7 dB (electrical) lower than the weakest LOS component received. For this reason only LOS components are considered in the simulations reported here (A similar approach is taken in [4]). In this case the (position dependent) channel bandwidth is limited by the relative delay and intensity between LOS components from different LEDs to each receiver. The greatest path length difference between the LOS components is when the receiver is at one corner of the room and is approximately 3m, corresponding to an approximate maximum delay of 10ns, or a bandwidth in the range of 100 MHz. This is in reasonable agreement with the detailed simulations in [4] which shows that bandwidth in a similar space is at least 90 MHz. Given the channel data rates are substantially less than this the difference between LOS components are ignored in these simulations and the DC channel gains [22] are used to describe the channel matrix H.

It is assumed that the system has N_T transmitters consisting of K LEDs arranged in a square array, and N_R receivers. The DC gain between transmitter i and receiver j, h_{ij} can be estimated by summing all the power reaching the jth receiver from the K LEDs in transmitter i,

$$h_{ij} = \left\{ \begin{array}{cc} \sum_{k=1}^{K} \frac{A_{rx}^j}{d^2{}_{ijk}} R_o(\phi_{ijk}) \cos(\varphi_{ijk}) & 0 \le \varphi_{ijk} \le \varphi_c \\ 0 & \varphi_{ijk} > \varphi_c \end{array} \right\}, \tag{2}$$

where $A_{rx}^j$is the receiver collection area for the jth receiver, d_{ijk} is the distance between the kth LED in ith transmitter and the jth receiver, ϕ_{ijk} is the emission angle, and φ_{ijk} is the angle of incidence of the light at the receiver, and φ_c is the receiver FOV. The H matrix is formed by the DC gains between each transmitter and receiver;

$$H = \begin{bmatrix} h_{11} & h_{1j} & \cdots & h_{1N_T} \\ h_{i1} & h_{ij} & \cdots & h_{2N_T} \\ \vdots & \vdots & \vdots & \vdots \\ h_{N_R1} & h_{i2} & \cdots & h_{N_RN_T} \end{bmatrix}, \tag{3}$$

At the receiver, the inverse of H can be used to obtain the estimated N_T transmitted signals.

D. Receiver

The receiver consists of an optical concentrator, followed by a detector and preamplifier. It is assumed that the concentrator gain is the theoretical maximum, and the receiver collection area A_{rx}^j is given by

$$A_{rx}^j = \frac{n^2}{\sin^2(\varphi_c)} A_{PD}, \tag{4}$$

where A_{PD} is the photodetector area and n is the concentrator refractive index. The received signal on the jth receiver r_j can be written

$$r_j = \gamma P_{LED} \sum_{i=1}^{i=N_T} h_{ij} t_i + \sqrt{\overline{i_{nj}^2}}, \tag{5}$$

where γ is the detector responsivity and $\overline{i_{nj}^2}$ is the mean square noise current at the input to the receiver preamplifier. For an individual receiver this is given by

$$\overline{i_{nj}^2} = 2e\gamma(P_{signal,j} + P_{ambient})B + i^2{}_{amp}B, \qquad (6)$$

where $P_{signal,j}$ is the average received communications power;

$$P_{signal,j} = P_{LED} \sum_{i=1}^{i=N_T} h_{ij}t_i, \qquad (7)$$

$P_{ambient}$ is the power received from ambient light (where$P_{ambient} = \chi_{amb}A_{rx}^i 2\pi(1-\cos(\varphi_c))$, B is the receiver bandwidth and i_{amp} is the preamplifier noise current density. In simulation a random number generator with the correct Gaussian statistics is used to generate an appropriate noise level which is added to the incoming signal.

Representing the received signal from all receivers as $R = [r_1, ...r_i....r_{N_R}]^T$ the received signal can be written $R = \gamma P_{LED}(H \bullet T) + N$ where $\bullet$ denotes matrix multiplication and $N = \left[\sqrt{\overline{i_{n1}^2}}, \sqrt{\overline{i_{n2}^2}}, ...\sqrt{\overline{i_{nN_R}^2}}\right]^T$.

The inverse of H can be used to generate an estimate of the transmitted signals T_{est}.

$$T_{est} = H^{-1} \bullet R, \qquad (8)$$

where H^{-1} is the inverse matrix of H and is already known at the receiver. Once estimates of the transmitted signal [14] are obtained these are low pass filtered and equalized if appropriate. The data streams are then combined to create a single received data stream, which is compared with the transmitted stream to obtain an estimate of the Bit Error Rate (BER). This is achieved by (i) aligning the transmitted and received data streams by cross-correlating to obtain the delay between them and aligning the waveforms by offsetting them by this delay (ii) integrating the received energy over a bit period (iii)using a maximum likelihood technique to obtain an estimate of the transmitted bits and (iv) comparing with the transmitted signal to obtain errors. A random sequence of 100 million bits is used to test the BER, which offers close to 100% confidence that the BER $< 10^{-6}$ for an error free sequence [23].

E. Non-imaging optical MIMO Simulation Results

A 4-transmitter, 4-receiver non-imaging system was simulated for the case of the white LED channel. Fig. 3 shows the distribution of the BER within a room. It can be seen that the system does not work in the central area and performance improves as the receiver moves outwards toward the corners.In the graphs shown in the paper the minimum BER shown is at this level to ensure this level of confidence.

For MIMO to operate the H matrix must be of full rank, and symmetry means that this is not the case in the center and along the axes of the room. It can be seen that as the matrix becomes less well conditioned the BER also increases, due to the difference in the coefficients being of the same order as the variation in noise. By rearrangement of the receiver geometry it may be possible to break the symmetry of this system and obtain correct operation at all positions, but it is likely that conditions will create some position at which it is not possible to break symmetry and create a full-rank matrix. For this reason the non-imaging case is not considered to be practical. In the next section an imaging system that overcomes these limitations is described.

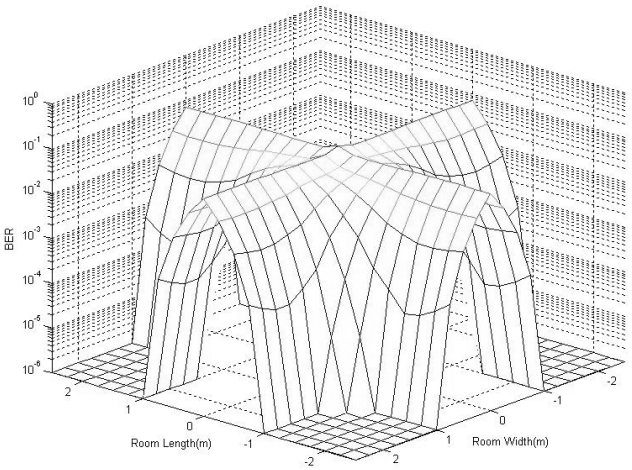

Fig. 3. BER room distribution for communications in a room using non-imaging optical MIMO model

III. Imaging Diversity Optical MIMO System

Fig. 4 shows a 4 channel visible-light indoor optical wireless system. An imaging receiver [16] is used in place of the non-imaging devices. Light propagates from the four transmitter LED arrays to the receiver as before, and each LED array is imaged onto a detector array, where images may strike any pixels or group of pixels on the array, and be in arbitrary alignment with them. Each pixel on the detector array is a receiver channel, and measuring the H matrix describing the optical connection between each pixel and each transmitter LED array allows the received signals to be separated as described in section II. In this paper it is assumed that the LED arrays form sharp images at the receiver, although the processing will likely be tolerant to a degree of misfocus or blurring and overlapping of the images of each transmitter array. This is because it does not rely on the signals from individual transmitters being spatially separate at the individual pixels, only that the H matrix is full-rank.

A. Imaging Diversity Optical MIMO Model

The approach follows that of the non-imaging case, with a modification of the channel matrix H_{image}. Each element is made up of two components and can be written

$$h_{image,ij} = a_{ij}h_i^{'} \qquad (9)$$

where $h_i^{'}$is the normalized power in the image of the ith LED array at the aperture of imaging lens when the receiver is at a particular position, and a_{ij} quantifies how much of this power falls on the jth receiver. $h_i^{'}$ can be written

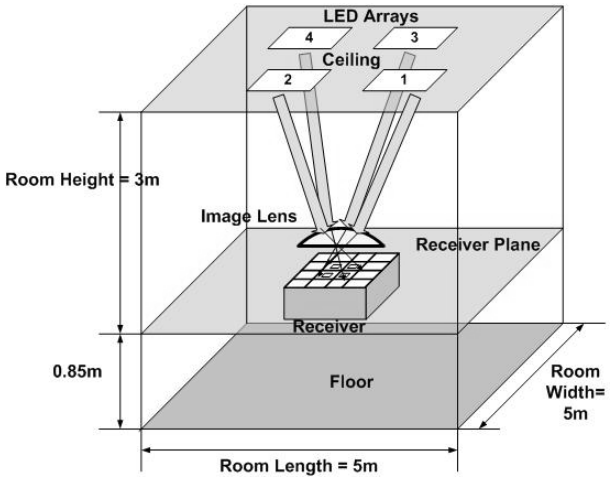

Fig. 4. Visible-light indoor imaging optical wireless system model

$$h_i^{'} = \left\{ \begin{array}{cc} \sum_{k=1}^{K} \frac{A_{rx}^{'}}{d_{ik}^{'2}} R_o(\phi^{'}{}_{ik}) \cos(\varphi^{'}{}_{ik}) & 0 \le \varphi^{'}{}_{ik} \le \varphi^{'}{}_{c} \\ 0 & \varphi^{'}{}_{ik} > \varphi^{'}{}_{c} \end{array} \right\}, \tag{10}$$

where $A_{rx}^{'}$ is the imaging receiver collection area, $d^{'}{}_{ik}$ is the distance between the kth LED in transmitter i and the center of the receiver collection lens, $\phi^{'}{}_{ik}$ is the emission angle, $\varphi^{'}{}_{ik}$ is the angle of incidence of the light at the receiver, and $\varphi^{'}{}_{c}$ is the receiver FOV.

An image of the ith transmitter forms on the receiver array, as shown in Fig. 5, and a_{ij} represents the proportion of the image area that falls of the jth detector pixel in the array;

$$a_{ij} = \frac{A_{is(s=j)}}{\sum_{s=1}^{s=N_R} A_{is}}, \tag{11}$$

where A_{is} is the area of the image of the ith transmitter on the sth detector pixel in the array. The position size of the images is determined by a geometric optical calculation, as described below.

B. Imaging Diversity Receiver

Fig. 5 shows the geometry of the imaging receiver in a room, with one of the LED arrays imaged to an area of the receiver plane via the imaging lens. In this analysis we use a paraxial optics approach, so that the system magnification is independent of the angle of incidence of the rays, and there is no image distortion. (More detailed analysis would likely be required for any practical optical system design.) The focal length L is determined by diameter D and image lens f-number $f_{\#}$, where $L = Df_{\#}$. The magnification of the system M is given by $M = d_z/L$ where d_z is the vertical distance from the receiver to the ceiling. A, B, C and D are the four corners of one LED array in the ceiling and $A^{'}$, $B^{'}$, $C^{'}$ and $D^{'}$ are the corresponding image coordinates, where $A^{'}B^{'} = MAB$, $B^{'}C^{'} = MBC$, $C^{'}D^{'} = MCD$, $D^{'}A^{'} = MDA$. This allows the position of the image and hence the coefficients a_{ij} to be determined as explained previously.

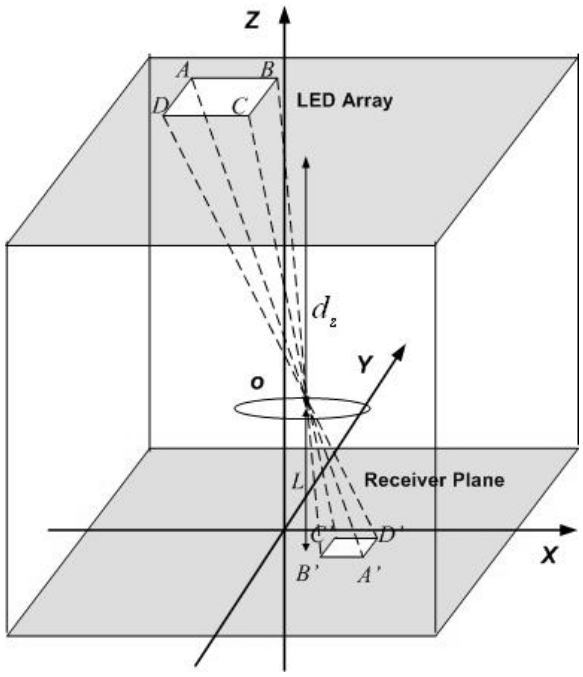

Fig. 5. Schematic of imaging calculation used to determine the position of the image of the LED arrays on the receiver

The size of the detector array must be large enough that the images of the transmitters fall on detectors for all receiver positions in the room. Fig. 6 shows the worst case when the receiver is in the corner of the room. For this

$$L_{rx} \approx \frac{2B_x}{M}, \tag{12}$$

where the dimensions are as shown on the diagram, and $L_{rx} \ll B_x$. Similarly

$$L_{ry} \approx \frac{2B_y}{M}. \tag{13}$$

Fig. 7 shows the schematic of the detector array for the receiver in the corner of the room. If the detector pixel size is L_{px} x L_{py} and $L_{px} > b_x$ and $L_{py} > b_y$ as shown in Fig. 7(a) then all the received signal falls on one detector and the signal cannot be recovered. However, if some of the signal is received by each of the detectors as in Fig. 7(b) the signal can be recovered. There is therefore a minimum pixel size that can be estimated using a similar technique for larger numbers of transmitters and receivers. It should be noted that there are always more receivers (detectors) than transmitters in order to ensure H is full-rank, so that a pseudo-inverse is used to estimate the transmitted data.

The receiver array collects ambient light from all parts of the room, and this creates unwanted photocurrent, so a threshold is set for each detector pixel, and if the received photocurrent is below this value then it is set to zero in the subsequent calculation. The maximum value is chosen as the maximum value for the particular simulation under consideration.

In this simulation, the threshold is set to be 10 times the maximum noise photocurrent from a detector pixel that is not illuminated by a signal, so that any pixels receiving only noise are set to zero. Without this threshold optical noise power

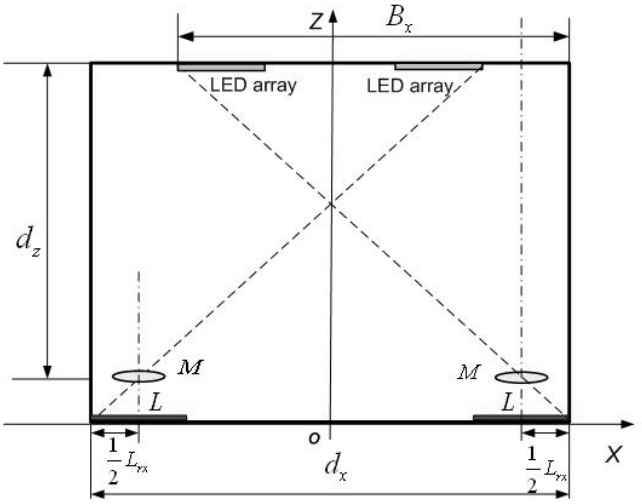

Fig. 6. Geometry of system with receiver at corner of room

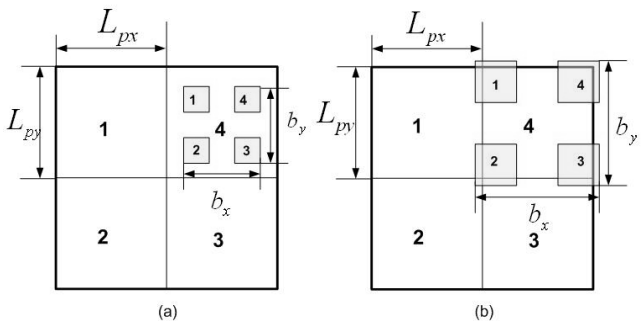

Fig. 7. The images on the detector array, (a)when $L_{px} > b_x$ and $L_{py} > b_y$ (b) when $L_{px} < b_x$ and $L_{py} < b_y$

would be received over an area $L_{rx}L_{ry}$, but this is reduced to an area where there is signal and noise present (so that the signal is over the threshold), given by $\sum_{i=1}^{i=N_T}\sum_{s=1}^{s=N_R} A_{is}$, so the ratio of these gives an approximate estimate of the drop in noise power received.

C. Simulation and Results

Table II shows the parameters used for the imaging simulations. Fig. 8 shows three different arrangements of LED arrays used in the simulations, where the total number of LEDs is fixed: (a) is used in a standard office, and (b) and (c) are cases with increasing numbers of transmitter arrays, where the spacing is designed to keep the illumination level at the walls the same as in the standard case (a). Table III shows details of these geometries. The collection area of the lens is determined by the minimum power levels at the receiver array to achieve the desired SNR and hence BER, and the f-number determines the focal length and indirectly the size of the detector array required. For each geometry, the BER is calculated for each receiver position within the communications plane.

D. Comparison of Different Transmitter Types

Transmitters that used the white, equalized white, and blue-filtered LED channels were investigated, using individual

TABLE II
PARAMETERS USED FOR IMAGING MIMO SIMULATIONS

Parameters	Values
Room size (WxLxH)	5 m x 5 m x 3 m
Number of LEDs arrays	4
Number of LEDs per array	3600(60*60)
LED array pitch	2.5 m
Vertical distance from ceiling to receiving plane d_z	2.15 m
LED pitch	0.01 m
Average transmitted power per LED(white/blue)	10/1 mW
Lambertian order m/Transmitter semi-angle	1/60 deg.
PD responsivityγ (white/blue)	0.4/0.1 A/W
Blue filter transmission	60%
Imaging lens f number$f_{\#}$	1
Imaging lens transmission	0.9
Pre-amplifier noise density [17]	5 pA/HZ$^{-1/2}$
Ambient light photocurrent [18]	10.93 A/m^2/Sr
Receiver Bandwidth B	0.7xNRZ-OOK data rate

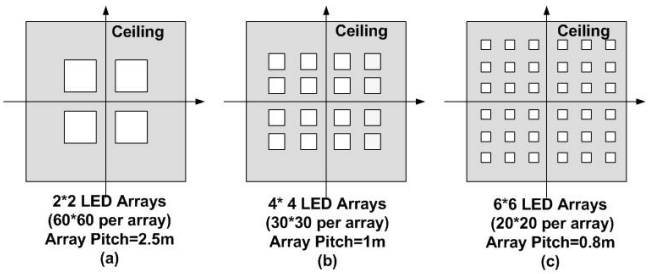

Fig. 8. LED arrangements for simulations

SISO channel rates of 12, 30 and 40 Mbits/s respectively. As mentioned previously for the equalized case there is an SNR penalty of approximately 18 dB due to the equalizer, and for the blue filtering there is a penalty of 36 dB.

Table IV, Table V and Table VI show the results of simulations, and the data rates available for different numbers of channels. In each case the size of the receiver is minimized so that an estimated BER of 10^{-6} is achieved at all points in the room. The BER at the edges of the room is worse than the center, as the received signal level is reduced, although it still meets the 10^{-6} target.

It can be seen that the blue channel is not suited to MIMO at high speed, as power in the blue component, filter losses and low responsivity lead to very large receivers in order to collect enough power. The equalized and white components have comparable performance in terms of receiver size and data rates, but for a specific data rate, the white LED based system requires more channels as the individual channel rate is lower. In terms of data rate performance the equalized channel has the potential to provide Gbit/s rates, albeit with a large receiver array.

IV. EFFECT OF MISALIGNMENT

The receiver can be rotated in the horizontal plane relative to the LED arrays, and it can also be tilted about the horizontal plane in both angular axes. The effect of rotation in the horizontal plane is briefly summarized in the following sections.

TABLE III
TRANSMITTER AND RECEIVER CHARACTERISTICS FOR PARTICULAR SIMULATIONS

LED illumination pattern	(a)	(b)	(c)
Transmitter arrays	2x2	4x4	6x6
Array pitch (m)	2.5	1	0.8
Full angle FOV (deg.)	124	126	130
Detector array size	4x4	8x8	12x12

TABLE IV
SIMULATION RESULTS FOR WHITE CHANNEL

LED illumination pattern	(a)	(b)	(c)
Number of channels	4	16	36
Data rate (Mbit/s)	48	192	432
Lens diameter (cm)	0.2	0.44	0.71
Detector size (silicon area) (cm)	0.74x0.74	1.68x1.68	3.05x3.05

TABLE V
SIMULATION RESULTS FOR EQUALIZED CHANNEL

LED illumination pattern	(a)	(b)	(c)
Number of channels	4	16	36
Data rate(Mbit/s)	120	480	1080
Lens diameter (cm)	0.44	0.80	1.38
Detector size(silicon area) (cm)	1.65x1.65	3.08x3.08	5.91x5.91

TABLE VI
SIMULATION RESULTS FOR BLUE CHANNEL

LED illumination pattern	(a)	(b)	(c)
Number of channels	4	16	36
Data rate (Mbit/s)	160	640	1440
Lens diameter (cm)	1.60	3.60	7.14
Detector size (silicon area) (cm)	6.0x6.0	13.77x13.77	31.4x31.4

A. Horizontal Rotation

The effect of horizontal rotation is shown in Fig. 9(a). It can be seen that if the receiver is in the corner of the room and rotated by 45 degrees then the detector array must increase in size by a factor of $\sqrt{2}$ relative to the unrotated case. The minimum size of an individual pixel is set by similar conditions as previously, and show in Fig. 9(b). This condition is that the images of two transmitters cannot fall completely on a single detector, but in this case the detector is rotated 45 degrees to the transmitter arrays, so that the minimum pixel size is reduced by a factor of approximately $\sqrt{2}$ compared with the unrotated case. There is a further constraint that the image of the illumination cannot fall symmetrically on the array. Together these lead to a receiver array $\sqrt{2}$ times as large with a minimum number of pixels approximately twice as large as the unrotated case. Table VII and Table VIII summarize the modified receiver designs for these cases and the data rates achievable.

B. Vertical Rotation

The receiver has a field of view that is set by the case when the receiver is at one corner of the room, but for positions closer to the center not all this field of view is required, so there is some tolerance to vertical rotation as long as the combined effect of rotation and the angle that light enters the receiver does not exceed the available field of view. Fig. 10 illustrates the case for the XZ plane (Y=0). For a particular position the rays enter at a maximum angle of ψ_x , so that a vertical rotation φ_x can be tolerated, as long as $|\psi_x + \varphi_x| \leq \varphi_{cx}$, where φ_{cx} is the receiver field of view for angles in the XY plane. For a particular position there are generally two limiting values of φ_x, corresponding to the receiver being rotated clock wise or counter-clockwise in a vertical direction, and these can be determined by straightforward trigonometry. Fig. 11 shows contours of allowed vertical rotation for different receiver positions in the room, where positive and negative represent clock and counterclockwise receiver rotations.

V. SYSTEM OPERATION

The simulations presented here have considered the potential for using MIMO processing to recover data, but any real system would have to measure the channel matrix assess its condition and perform the required mathematical operations, as is the case for RF systems. Preliminary MIMO experiments [24] indicate that channel estimation is relatively straightforward. In the experiments a training sequence is sent successively from each transmitter and measurements of the received signal made at each receiver. DC channel gains can be estimated from the relative amplitudes of each waveform, and the real data is then transmitted and recovered. It might also be possible to use the frequency range below the minimum frequency of the (typically) AC coupled optical receiver as a separate measurement channel, and send pilot tones to estimate the channel at the same time data is transmitted. The baseband nature of the channel, and the intensity transmission of data make the characteristics of these systems distinct from RF examples, and methods of channel estimation is therefore an area of future investigation.

The simple matrix inversion and multiplication used to obtain an estimate of the transmitted data is susceptible to noise, and computationally inefficient compared with many of the advanced RF techniques in use [9], and there are likely to be substantial gains to be made with use of some of these, and this is an area for future research. For the limited cases considered here the full rank of the matrix is assured by the design-essentially the minimum detector pixel size which means that transmitter signals always fall on more than one detector. As the transmitter images are separate a sufficiently small detector pixel size will always ensure full rank for a particular magnification. However, this analysis assumes ideal imaging, and it may not be practical to increase the number of detector pixels, so the case where the matrix is deficient must be considered in any practical system design. A simple solution would be to reduce the number of independent transmitters until a full rank matrix was available. This would reduce the capacity but increase channel signal to noise ratio. Channel estimation and data transmission, with the possibility of adaptation if the matrix is not full rank, all require varying degrees of coordination of the transmitters and receivers, and the details of this are beyond the scope of this paper. At its simplest coordinated transmission of data and training sequences for channel estimation, as used in preliminary experiments, would allow MIMO broadcast.

TABLE VII
RECEIVER DESIGNS FOR (A), (B) AND (C) GEOMETRY STRUCTURES WHEN $\theta_h = 45^o$

LED illumination pattern	(a)	(b)	(c)
Number of channels	4	16	36
Array pitch (m)	2.5	1	0.8
Full angle FOV (deg.)	124	126	130
Detector array size	5x5	13x13	23x23

TABLE VIII
SIMULATION RESULTS USING WHITE LED WHEN $\theta_h = 45^o$

LED illumination pattern	(a)	(b)	(c)
Number of channels	4	16	36
Data rate (Mbit/s)	48	192	432
Lens diameter (cm)	0.2	0.44	0.71
Detector size (silicon area, 45^o) (cm)	1.15x1.15	2.39x2.39	4.32x4.32

VI. CONCLUSIONS AND FUTURE WORK

An imaging diversity receiver, combined with MIMO processing techniques allows 'alignment free' high data rate communications.

The most power efficient scheme is to use the white LED channel, as the power penalties in using the higher bandwidth equalized and blue filtered channels are greater than the simple power splitting involved in using multiple white channels. However, in practical cases the complexity of the large number of channels may make a smaller number of high bandwidth channels more attractive. At present the receiver imaging lens and detector array size are large for some configurations, and are not likely to be practical for some applications.

In both cases data rates from several hundred Mbit/s to 1Gbit/s can be achieved.

The systems analysed in this paper to some extent represent the 'limiting cases'-that of imaging and non-imaging, and it may be that some hybrid system offers a means of creating a system that can use a more compact receiver array. This is worthy of further work, as it is an open question as to what optical system creates the best optical MIMO system.

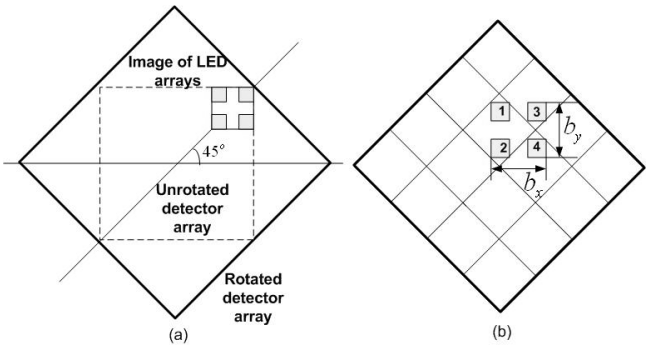

Fig. 9. (a) Effect of rotation on the size of detector array. (b) Effect of rotation on the size of an individual detector pixel.

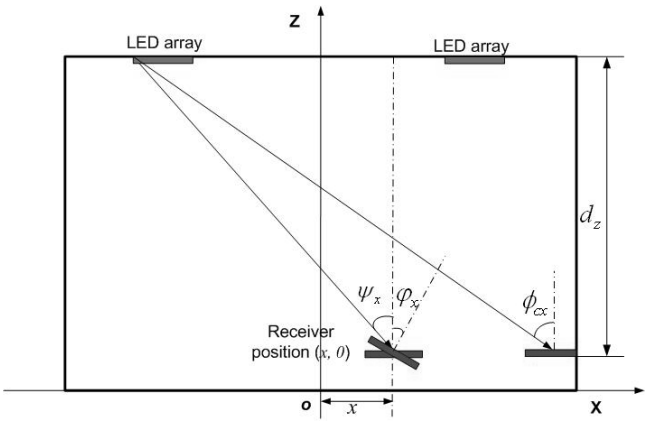

Fig. 10. Receiver positioned at the right corner and one particular position (X>0) of the room (Y=0).

REFERENCES

[1] T. Komine and M. Nakagawa,"Fundamental analysis for visible-light communication system using LED lights", *IEEE Trans. Consum. Electron.*, vol. 50, pp. 100-107, Feb. 2004.

[2] VLCC, "Visible Light Communications Consortium," 2008.

[3] J. G. K.-D.Langer, O.Bouchet, M.El.Tabach, J.W.Walewski, S.Randel, M. Franke, S. Nerreter, D.C. O'Brien, G.E.Faulkner, I.Neokosmidis, G. Ntogari and M.Wolf, "Optical wireless communications for broadband access in home area networks,", 10th Anniversary International Conference on Transparent Optical Networks, 2008, Athens, Greece, vol. 4, pp. 149-154.

[4] J.Grubor, S.Randel, K.D.Langer and J.W.Walewski, "Broadband information broadcasting using LED-based interior lighting," *J. Lightw. Technol.*, vol.26, no.24, pp.3883-3892, 2008.

[5] D.C. O'Brien, H. Le-minh, G.E. Faulkner, O. Bouchet, M. El.Tabach, M. Wolf, J.W. Walewski, S. Randel, S. Nerreter, M. Franke, K.-D. Langer, J.Grubor,T.Kamalakis, "Home access networks using optical wireless transmission," in *Proc. IEEE PIMRC*, Cannes, France, 2008, pp.1-5.

[6] IEEE, "IEEE 802.15.7 WPAN Visual Light Communication Study Group," 2008.

[7] Occupational-Safety-and-Health-Branch-Labour-Department, "Simple Guide to Health Risk Assessment - Office Environment Series OE 2/99," 1998.

[8] L. Zeng, D. O'Brien, H. Le-Minh, L. Kyungwoo, J. Daekwang, and O. Yunje, "Improvement of Date Rate by using Equalization in an Indoor Visible Light Communication System," in *Proc. IEEE ICCSC* , 2008, pp. 678-682.

[9] D. Gesbert, M. Shafi, Da-shan-Shiu, P. J. Smith, and A. Naguib, "From theory to practice: an overview of MIMO space-time coded wireless systems," in *IEEE J. Sel. Areas Commun.*, vol. 21, pp. 281-302, Apr.2003.

[10] S. G. Wilson, M. Brandt-Pearce, Q. Cao, and J. Leveque, "Optical MIMO transmission using Q-ary PPM for atmospheric channels," in *Signals, Systems and Computers, 2003. Conference Record of the Thirty-Seventh Asilomar Conference on* , vol.1, pp. 1090- 1094, Nov. 2003.

[11] Jivkova-S, Hristov-Ba, and Kavehrad-M, "Power-efficient multispot-diffuse multiple-input-multiple-output approach to broad-band optical wireless communications," in *IEEE Trans. Veh. Technol.*, vol. 53, pp. 882-889, May 2004.

[12] Hranilovic-S and Kschischang-Fr, "A pixelated MIMO wireless optical communication system," in *IEEE J. Sel. Topics Quantum Electron.*, vol. 12, pp. 859-74, Jul.-Aug. 2006.

[13] Garfield-M, Chao-Liang, Kurzweg-Tp, and Dandekar-Kr, "MIMO space-time coding for diffuse optical communication," in *Microwave and Optical Technology Letters*, vol. 48, pp. 1108-10, Jun.2006.

[14] D. C. O'Brien, "Indoor optical wireless communications: recent developments and future challenges," in *Free-Space Laser Communications IX*, San Diego, CA, USA, 2009, pp. 74640B-12.

[15] A. G. Kirk, "Free-Space Optical Interconnects,", in *Optical interconnects : the silicon approach*, L. Pavesi and G. G. Guillot, Eds. Berlin: Springer, 2006.

[16] J. M. Kahn, R. You, P. Djahani, A. G. Weisbin, B. K. Teik, and A. Tang, "Imaging diversity receivers for high-speed infrared wireless communication," in *IEEE Commun. Mag.*, vol. 36, pp. 88-94, 1998.

[17] D. C. O'Brien and M. Katz, "Optical wireless communications within fourth-generation wireless systems," in *J. Optical Networking*, vol. 4, 2005.

[18] A. J. C. Moreira, R. T. Valadas, and A. M. de-Oliveira-Duarte, "Optical interference produced by artificial light," in *Wireless Networks*, vol. 3, pp. 131-40, 1997.

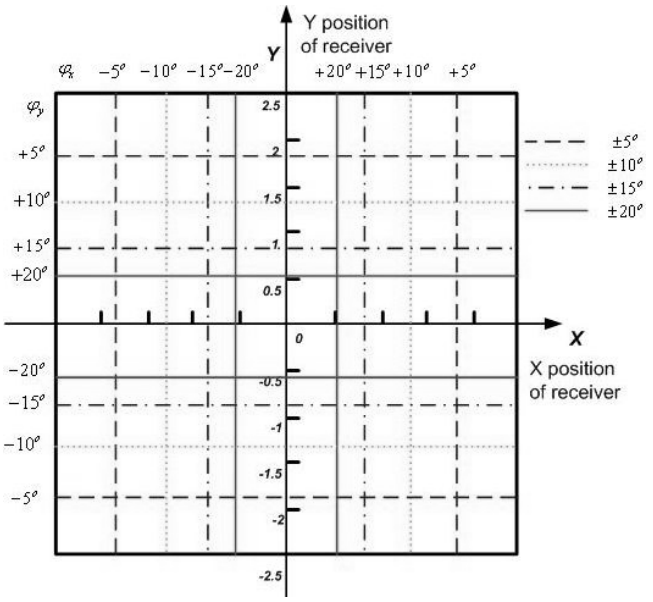

Fig. 11. Plan view of room showing allowed vertical misalignment for different positions within the room.

[19] Luxeon Star, Application brief AB20-3, www.luxeon.com, 2006.
[20] D. C. O'Brien, H. Le-Minh, G. Faulkner, L. Zeng, K. Lee, D. Jung and Y. Oh, "High-Speed Visible Light Communications Using Multiple-Resonant Equalization," in *IEEE Photonics Technol. Lett.*, vol. 20, no.15, pp. 1243-1245, 2008.
[21] G. W. Marsh and J. M. Khan, "50-Mb/S Diffuse Infrared Free-Space Link Using on-Off Keying with Decision-Feedback Euqalisation," *IEEE Photonics Technol. Lett.*, vol. 6, pp. 1268-1270, 1994.
[22] J. M. K. J.R. Barry, W. J. Krause, E. A. Lee and D.G.Messerschmitt, "Simulation of multipath impulse response for indoor wireless optical channels," *IIEEE J. Sel. Areas Commun.*, vol. 11, No.3, pp. 367-379, 1993.
[23] M. Mueller, R. Stephens and R. McHugh, "Total Jitter Measurement at Low Probability Levels, Using Optimized BERT Scan Method," in *Designcon 2005*.
[24] D. C. O'Brien, S. Quasem, S. Zikic, and G. E. Faulkner, "Multiple input multiple output systems for optical wireless: challenges and possibilities," in *Free-Space Laser Communications VI*, 006 , vol. 6304, pp. 630416.1-630416.7.

Lubin Zeng received her BSc(2003) in Electronics Engineering from East China Normal University, and then obtained an MSc(2004) in Communications and Signal Processing from Imperial College, University of London. She is currently studying for the D.Phil degree in the Department of Engineering Science at the University of Oxford. Her research interest is indoor optical wireless communications.

Dominic O'Brien is a Reader in Engineering Science at the University of Oxford, and leads the optical wireless communications group. He gained MA(1991) and PhD (1993) Degrees from the Department of Engineering at the University of Cambridge. From 1993-1995 he was a NATO fellow at the Optoelectronic Computing Systems Center at the University of Colorado. His current research is in the field of optical wireless systems. He is the author or co-author of approximately 130 publications or patents in the area of optics and optoelectronics.

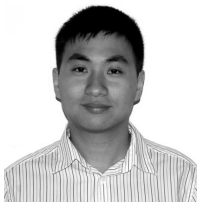

Hoa Le Minh was born in Hochiminh city, Vietnam. He obtained his first degree at Hochiminh city University of Technology in 1999. He was then appointed as a lecturer in Telecommunications division at the same university. He received his MSc degree from Munich University of Technology, Germany, in 2003. At the same time he was a research assistant in R&D Optical Network department, Siemens AG, Munich, Germany. Hoa received his PhD in 2007 from Northumbria University, UK, in Optical Communications. He is now with the University of Oxford, UK, working in indoor visible light communications and Gigabit infra-red cellular communications.

Grahame Faulkner is a Research Assistant in the Department of Engineering Science. He received his B.Sc. honours in physics and microelectronics from Oxford Brookes University. He has over 10 years of experience in the field of optical wireless communications, optical interconnects and optoelectronic integration.

Kyungwoo Lee Telecommunication R&D Center, Samsung Electronics Co. Ltd , Suwon, South Korea (phone: +82 (0)312795575, fax: +82 (0)312795255, email: kyungwoo72.lee@samsung.com.

Daekwang Jung Telecommunication R&D Center, Samsung Electronics Co. Ltd , Suwon, South Korea (phone: +82 (0)312795575, fax: +82 (0)312795255.

YunJe Oh Telecommunication R&D Center, Samsung Electronics Co. Ltd , Suwon, South Korea (phone: +82 (0)312795575, fax: +82 (0)312795255.